Carbon Dust—Its Short-Term Influence on Potroom Operations During Anode Change

Matthias Dechent, Mark Philip Taylor, Richard Meier, Lea Tiedemann, Markus Meier, and Bernd Friedrich

Abstract

Carbon dust refers to carbon particles, originating from carbon inputs into the smelting process like anodes, that float on top of the bath, below anodes or suspended in the bath. The phenomenon has a deleterious effect on the specific energy consumption of cells and can lead to anode deformations, hot cells out of the process window and stoppage of cells. Trials were conducted in the TRIMET Hamburg Smelter focusing on the effect of dust at anode changes. The conditions were chosen to be best and worst practice as assessed by a visual carbon dust assessment in the tap hole. Contrasting with published literature, there was no relation in the experiments between spike formation and carbon dust in anodes after 8 h. Anodes set in cells with a high carbon level in the tap hole did not behave differently when compared to anodes with a low carbon dust content in the tap hole. Samples obtained from the frozen bath layer underneath the anodes showed carbon contents in the range of 0.0315–6.29%.

Keywords

Carbon dust • Spike • Potroom operation

M. Dechent (✉) · R. Meier · L. Tiedemann
TRIMET Aluminium SE, Aluminiumstraße 1,
21129 Hamburg, Germany
e-mail: matthias.dechent@trimet.de

M. P. Taylor
University of Auckland, Auckland, New Zealand

M. Meier
R&D Carbon Ltd., P.O. Box 362 3960 Sierre, Switzerland

B. Friedrich
IME RWTH Aachen, Intzestraße 3, Aachen, Germany

Introduction

Carbon Dust

Carbon dust refers to small carbon particles, which are located in the electrolyte of an aluminium reduction cell [1–3]. Older sources refer to carbon slough [4] or carbon foam [5], which refers to a mixture of carbon particles of various sizes within the electrolyte in an aluminium reduction cell.

Carbon dust is considered one of the most important impurities in electrolytic bath for the aluminium electrolysis, especially, as an unwanted part. The carbon particle sizes can vary between microns and centimetres [6]. The distribution in the open bath is also depending on the depth of the samples taken from the bath [6] or on the positioning within the cell [7].

A cell can be considered to have carbon dust or to be dusty, if one or more of the following indications are true: carbon particles floating on top of open bath surface or opened tap hole, blackened anode cover material close to point feeders and tap hole, yellow burning flames, a high content of carbon in bath samples, anodes with carbon trapped underneath or within frozen bath [8, 9].

Carbon Dust Formation

Carbon dust has several formation mechanisms in and outside of the aluminium electrolysis cell. Inside the cell, there are the mechanisms of selective reactivity of the anodes due to a differential reactivity within the anodes [10] or pieces of carbon breaking off the anode [11] and cathode wear [12, 13]. Outside of the cell, carbon particles from anodes are crushed in the anode cover material plant and recycled to the cells as fresh anode cover material [2, 14].

Selective oxidation can occur with oxygen from the ambient air or from CO_2. While air reactivity is happening on the vertical sides of the anodes and the anode slots [15]

L. Perander (ed.), *Light Metals 2021*, The Minerals, Metals & Materials Series,
https://doi.org/10.1007/978-3-030-65396-5_55

and can be limited by use of proper anode cover material [16], CO_2 reactivity is depending on the temperature and the anode properties related to reactivity [17, 18]. Both CO_2 and air reactivity are related to the anode and cell temperature. While the temperature at the anode working surface is close to the cell temperature at around 960 °C, the anode side and top temperature is depending on the anode geometry and the anodes thermal conducting properties [19]. The top temperature is depending on the anode cover composition, the carbon to stub connection and its heat generation [20] and the anodes' thermal conductivity.

Air reactivity is depending on the temperature. According to Fischer [18], the air burn rate can be at 1 mm/h at 550 °C and the rate doubles with a temperature increase of 30 °C. The top anode temperature reaches 550 °C only after 42.5 h [19], while the bottom temperature reaches 800 °C after 12 h [21]. Sadler [22] discusses the formation of carbon dust from the sides due to carboxy attack on the part of the anode, which is submerged into the electrolyte. No electrolyte penetrated the samples in Sadlers study, indicating oxidation of the binder matrix due to the CO_2 in the anode itself. The CO_2 on the working surface has little time to further oxidize the particles. Also, electrochemical attack would then preferentially remove the protruding particles, which are left after the CO_2 attack [22].

Both reactivity with CO_2 and air can be reduced with coatings, for example with boric acid [23]. Coating anodes with liquid aluminium spray coating, has been a method especially used in the past, the concept of aluminium coating however was improved by EGA by using an aluminium thermal spraying technology in 2018 [24]. The old Al spraying method is still used at the Hamburg smelter due to the height of the anodes out of the cavity.

Spikes

Spikes are anode deformations or protrusions. Depending on the literature source, there are two sub-categories [25]: spikes due to solid bath underneath the anode or a non-liquid mixture of alumina and bath referred to as muck or sludge [26] and carbon protruding away from the anode surface (normally downward). These carbon protrusions can either be not-reacted carbon, also called cones [7], or carbon pieces and particles baked/sintered back to the anode. Odegard was able to create protrusions from aluminium carbides in a laboratory setup [27]. Zoukel repeated those trials in 2009 [12].

An uneven anode surface has several effects: if the protrusions are non-conducting for electricity, the working surface is reduced which leads to a higher resistivity for that anode due to the smaller available surface. Depending on the size of the muck spikes, the bath movement can also be hindered, leading to local changes of alumina concentration.

If the particles or protrusions are conducting current, they short the electrolysis process and the current is only "used" to heat up the spike. Solbu found local temperatures of up to 1400 °C ± 100 °C in conducting spikes in laboratory cells [28]. If the carbon part is then extending into the metal, according to Odegard [25] the electrodeposition of carbon from aluminium carbide starts right away, as the solubility of Al_4C_3 is very low in metal. The deposition rate, seemed to be related to low alumina concentrations, as the CO_2 evolution is reduced and there is less motion of the bath. Pietrzyk [3] found, that the alumina concentration close to trapped carbon is lower compared to other regions of the cell, which can lead to anode effects with a maximal voltage of 15 V [29]. After an anode effect, the electrodeposited carbon appeared to be gone in the trials of Odegard [27].

Anode Change

Anode change is a fundamental operation in an aluminium electrolysis cell, as the carbon anode is consumed during the electrolysis of alumina. The operation can upset the heat balance and influence the temperature of a cell locally [21, 28, 30]. The theoretical minimum carbon consumption to produce a ton of aluminium is 334 kg C/t Al [11]. However, due to other reactions a low number for net carbon today is at 400 kg C/t Al [31], having increased since to the implementation of slotted anodes by 5–30 kg C/t Al [15]. Depending on the cells' and anodes' dimensions, anodes have to be replaced every 22–32 days [32].

Anode Change Leading to Spike Formation

Anode change has been named as one cause for spike formation, especially in relation with carbon dust. Ali [33] identifies the freeze underneath newly set anodes as one of the spike mechanisms. During a carbon dusting crisis, the Egyptalum plant checked anodes a few hours (between 60 and 585 min) after anode change to find frozen bath underneath the anodes [33]. Wai-Poi [34] shows, that most spikes at the Voerde plant are found after six days, while in Ali's [33] study about 65% of spikes were found in between days 12 and 24 for a 30 day anode rota time. Antille [35] shows the influence of anode change on the magnetics, noise, and cell stability. Aune [21] discusses the temperature impact of anode changes, leading to temperatures of up to 1080°C inside an anode with spikes. Peterson [20] discusses different setting heights and the heat up for lower anodes.

Hypothesis

Combining the above information leads to the question: Is there a certain set of parameters leading to spike formation during anode change? And do these spikes form especially during the first hours of operation with a new anode?

The present study investigates parameters leading to spike formation within the first hours of anode setting in the Reynolds P19 cell technology, operated at 184 kA.

Experimental and Results

Methodology

Several studies have used measurement systems for carbon dust, which are observation based [36, 37]. Gudmundsson [36] describes an evaluation system with three levels used in Nordural in order to evaluate the amount of carbon dust. The evaluation is conducted at the tap hole. A cell with no visual carbon dust at the tap hole is a level 1 cell. Level 2 cells have carbon dust; however, the amount of dust can be scooped out at one attempt. Level 3 has more carbon dust than level 2, repeatedly coming back into the tap hole after being scooped out. Figure 1 shows the pictures from the reference document during the trials. Other evaluation systems and their efficiency have been tested [37].

In order to measure the anode current during and after anode change, the voltage drop between two points of the conductor, in this case the anode rod on the anode beam is measured [38]. For the 24 h measurement, the voltage should be between 3.0 and 4.5 mV in order to not be adjusted. In general, measurements of above 6.5 mV are considered abnormal during normal operations (not after 24 h) and those anodes are taken out to be checked.

During the experiments, bath samples were taken from the tap hole on the tap end of the cell during the evaluation of the carbon dust index. Sampling tongs were submerged after preheating to a depth of 10 cm below the bath surface, then opened and closed. The closed tongs were opened 5 min after sampling in order to reduce the temperature of the samples to reduce further reactions. The samples were then cooled down and stored in a container free of humidity until analysis.

The samples of frozen bath attached to the bottom of anodes were hammered off the surface during the anode check.

Samples were analysed by the XRD and LECO method.

In order to evaluate and measure the thickness of the frozen bath and the surface covered by bath, pictures were taken with a reference steel frame. The reference was then used to use a mesh of 5 cm × 5 cm squares. Figure 2 shows an example of this method.

Experimental Setup

Ali [33] and other show the freeze underneath freshly set anodes could lead to spike formation. Wai-Poi [34] mentions carbon dust as one of the factors leading to spikes.

In order to evaluate the short-term effect of anode change on the spike formation, cell conditions and working quality were taken into account.

Two anode change parameters were found to influence the spike formation in the literature review, and these were controlled during the present experiments along with the carbon dust state of the cell:

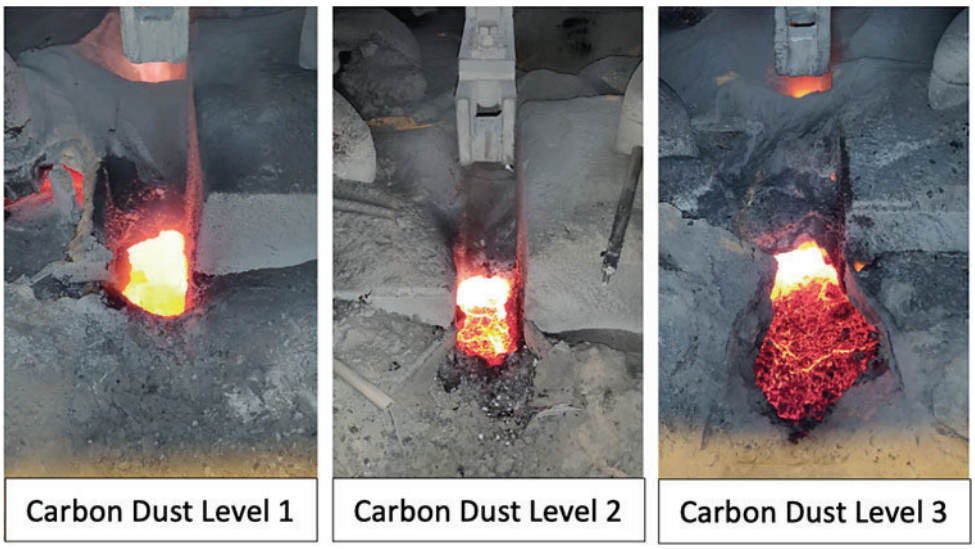

Fig. 1 Carbon dust levels in the tap hole, as used in Hamburg—Pictures for reference; Left: Carbon dust level 1, with no visual carbon dust in the tap hole; middle: Carbon Dust level 2, low quantities of carbon dust are visual, but can be scooped out in one pass; right: Carbon Dust level 3, higher carbon dust quantity than in level 2, cannot be scooped out in one pass. (Color figure online)

Fig. 2 5 cm by 5 cm grid for measurement of thickness and position of frozen bath layer underneath anode after the experiment's duration, Cell 239, anode K/8; Carbon Dust index 1/2, no pacman, anode set too low, duration 2 h. (Color figure online)

- The setting height of the anode is important for the current pickup during the heat-up [21, 35, 39, 40]. If the anode is set too low, it disturbs the magneto-hydrodynamic field in the cell. If the anode is set too high, the time until the current is picked up increases and therefore, the anode current distribution is disturbed over a long period.
- The use of a pacman, with is an excavator shovel on the pot tending cranes, for the cavity cleaning is a factor leading to a better working quality and better cell performance after anode change. Also, the number of cavity scoops taken in the cell could have an influence. However, the parameters for these experiments were set to be no cleaning at all, or cleaning with normal SOP, which means, the excavator has to be completely closed, there are no more large lumps.
- The carbon dust level assessed in the tap hole is the third factor in the experiments. In order to have a clear measure for dust state, the state is either level three or less, which means, the cell has a significant amount of dust in the tap hole or not.

During a period of three weeks, 30 anodes were changed according to the given parameters. Table 1: 8 Parameter combinations shows the actual number of experiments and trials. In order to test the time dependency, the anodes were checked after 2, 4, or 8 h. With the combinations, there were a "best case", "best case with carbon dust", and "worst case" scenario, depending on the factors used for the experiments. The worst case is conducted on a cell with level 3 carbon dust, no use of pacman and the anode was set too low. This should be the anode setting combination most likely to lead to spike.

Corner Anodes were excluded from the trials. The cells' bath temperatures were within the normal operating window, no cells with disconnected collector bar were tested.

Results and Discussion

The measurements of freeze under anodes showed the following:

- Observations on anodes with 8 h duration had no frozen bath layer underneath the anode.
- The maximum heights of 15 cm freeze are measured on the anodes from trials without cavity cleaning. This is independent of the carbon dust level of that cell. Figure 3 shows the measurements of the maximum height of the spike formed.
- With a longer duration after the anode change, the height of the frozen bath decreases from a median of 9 cm for cells with low carbon dust after 2 h, to 5 cm after 4 h,
- The cells with higher carbon dust level move their median from 6 cm after 2 h to 5.5 cm after 4 h. The skimming (using the pacman) actions lead to a median of 5 cm of height for trials that lasted 2 to 4 h, regardless of their tap hole carbon dust levels. However, a no skimming action shifted the median to 7 cm for carbon dust level 3 and to 11.5 cm for lower amounts of carbon dust in the tap hole.

The average ACD (anode cathode distance) for cells in Hamburg is on average between 42 and 45 mm, which leads to the hypothesis, that the protrusions of frozen bath are extending well into the metal pad. Samples taken from the frozen bath layer showed metallic spheric aluminium inclusions with a diameter of up to 15 mm, verifying the hypothesis.

None of the anodes during the experiment showed a spike within its operating time of 27 days. Since spikes are always an infrequent event, the absence of spikes during the 30 experiments is perhaps unsurprising.

The measurement of the total cross-sectional area of freeze covered in the steel grid is an indicator of the volume

Table 1 8 Parameter combinations of 3 controlled variables, which are conducted with different durations. Uneven chiffres are with Carbon Dust Level 1 or 2, even chiffre are conducted on cell with carbon dust level 3 in the tap hole. While chiffres Sp1, Sp2, Sp5, Sp6 are set on the correct height, Sp 3, Sp4, Sp7, and Sp8 are set too low. Sp 1, Sp2, Sp3, and Sp4 are using the pacman for Skimming, Sp5 to Sp8 are No Skimming experiments

	Chiffre	2 h	4 h	8 h	Sum
CD level 1 or 2	Sp1 (“best case”)	1	2	1	19
	Sp3	1	2	1	
	Sp5	3	1	1	
	Sp7	2	2	2	
CD level 3	Sp2 (“best case” with dust)	1	2	0	11
	Sp4	1	1	0	
	Sp6	1	1	0	
	Sp8 (“worst case”)	1	2	1	

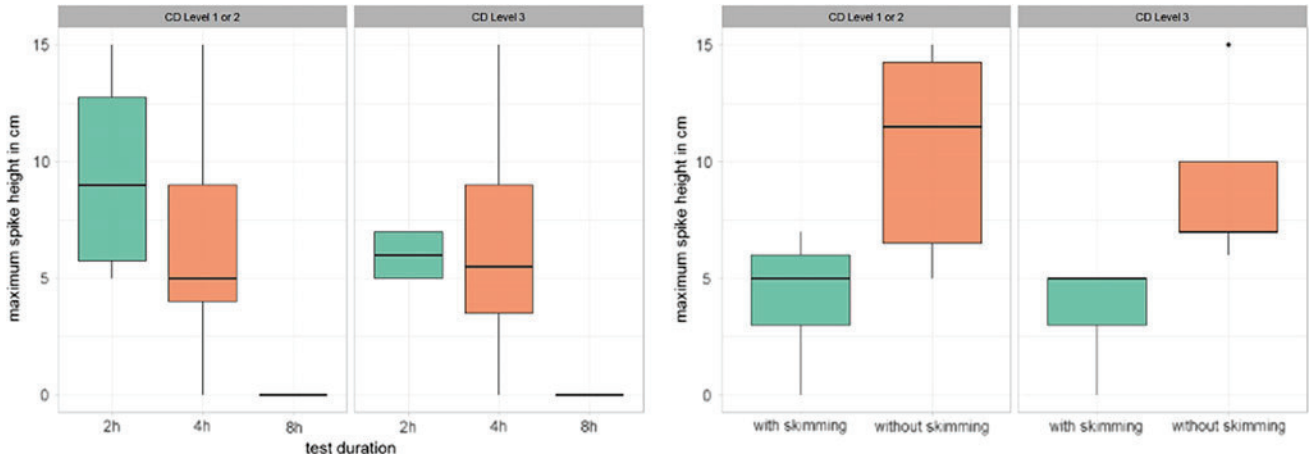

Fig. 3 Maximal spike height in cm, left: boxplot for the three durations of 2 h, 4 h, and 8 h, split for carbon dust levels 1 or 2 and 3. None of the 8 h experiments shows frozen bath underneath the anode; right: boxplot for the parameter No Skimming and Skimming, values for 8 h trials are not included, the median is for all carbon dust levels at 5 cm, if Skimming was applied, and is higher for No Skimming actions for low amounts of carbon dust assesses at the tap hole. (Color figure online)

of freeze under the anode. This was measured here to assess, whether the frozen bath from cells with a higher carbon dust level in the tap hole show a different distribution of the bath, or a different mass. As the total volume covered for experiments with an 8 h duration was nil, the data was excluded from further analysis. The median for carbon dust level 1 and 2 is 28 boxes covered, for carbon dust level 3 it is at 25 boxes. The spread for the carbon dust level 3 is considerably higher in comparison with carbon dust level 1 and 2, with the 25% quartile at 10 and the 75% quartile at 32.5 boxes. Figure 4 shows the measurement of the total volume of the frozen bath.

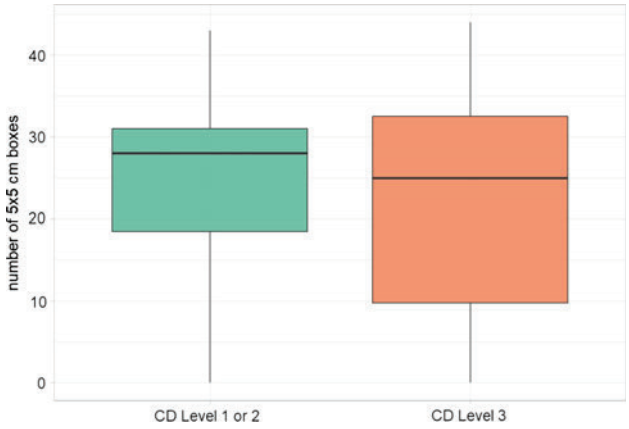

Fig. 4 Boxplot of total volume measurements, separated for Carbon dust level 1 or 2 and 3; data for 8 h trials has been excluded, as the area after 8 h was null. The median for level 1 or 2 is 28 boxes, while the median for level 3 is 25 boxes. However, the 25% and 75% quantiles for carbon dust level 3 show a higher spread of the data. (Color figure online)

Visual Inspection of Frozen Bath Layer

In order to understand the initial formation of protrusions during anode change, the frozen bath layer samples are

visually inspected. One would expect frozen bath with carbon inclusions for carbon dust level 3 and on cells with no skimming possibly particles from anode cover material, which falls into the bath during anode change.

Figure 5 shows two experiments with carbon dust level 3, but different appearances. The sample shown in the top part of the figure shows a line separating two different layers of bath. The first layer shows a high amount of carbon particles in different sizes. Close to the anode working surface, the particles are small, and the colour of the bath is black suggesting a higher carbon content of fine dispersed particles. Carbon particles with a bigger size are close to the interface with the second frozen layer. The maximum size of these particles is 3 mm, which is the smallest size of the coarse coke and butts particles from the anode formulation [41].

The lower layer of bath is clear and white. It appears to be mostly pure bath, although the pacman was not used during this experiment. The carbon content of the frozen bath sample taken as a combination from both layers is analysed with 1.25% C, while the sample taken in the tap hole has a carbon content of 0.0273% C. The bottom part of the figure shows a sample from a trial with the same duration, carbon dust level and the anode set too low but with the anode hole skimmed properly. Two layers are visible; the second layer appears already partially melted away. The upper layer has a grey color with black carbon particle inclusions with a maximum particle size of 2 mm. The lower layer does not show the same clear, white color, which was found in the other sample. The frozen bath layers analysis (combined in one sample) shows a carbon content of 1.34% C, the sample from the tap hole 0.0176% C.

The frozen bath samples in Fig. 6 left and right have the highest Carbon content in the frozen bath samples from all 30 trials. On the left the anode has a carbon dust level of 1 or 2, no skimming action, anode was set too low. The carbon content of the frozen bath layer is at 5.48% C, the bath sample in the tap hole is 0.0401% C. The visual inspection shows no clear distinction between layers. Big carbon particles are visible, with the largest at a 25 mm diameter. The piece could be a piece of the old. The sample on the right side includes many smaller carbon particles, with the biggest having a diameter of approximately 10 mm. These could be individual particles from the different fractions from the anode formulation. The experiment has a carbon dust level 3, no skimming action was performed and the new anode was set on the correct height. The Carbon content of the bath sample at the tap hole was at 0.0318% C, the frozen bath sample at 6.29% C the highest carbon concentration of all experiments.

The frozen bath sample for a “best case” anode change, which is the anode change according to standard procedure and with a carbon dust level 1 or 2 assessment shows two layers with big pores and compared to the other samples, extreme porosity. The lower layer includes layers of fine

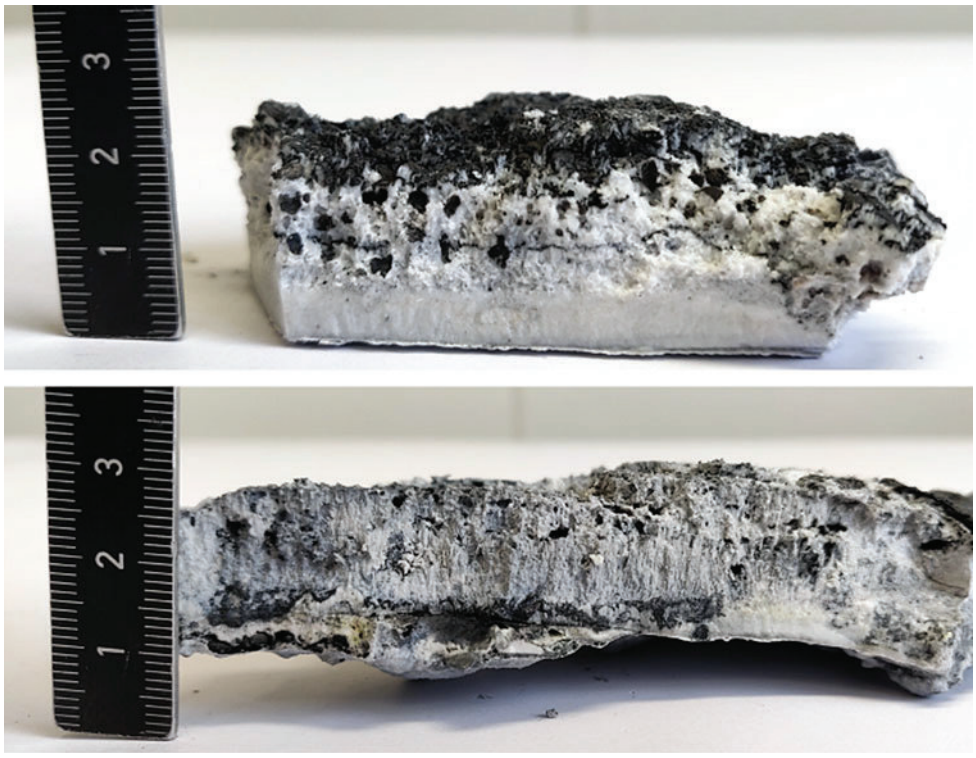

Fig. 5 Frozen bath samples, orientation as in cell (anode above, electrolyte below): top: 023-Sp8-2-01, Cell 129, anode 8, Cell with Carbon dust level 3, No Skimming, anode set too low, 2 h duration, carbon content in bath sample from tap hole: 0.0273% C, in spike sample: 1.25% C; bottom: 026-Sp4-2-01, cell 158, anode D, cell with carbon dust index 3, anode set too low, Skimming, Carbon content in bath sample from tap hole: 0.0176% C, in spike sample: 1.34% C

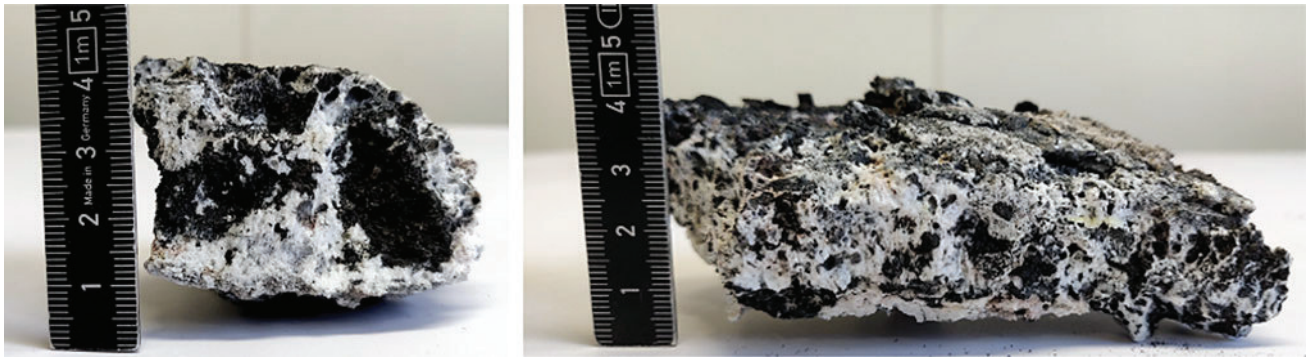

Fig. 6 Frozen bath sample underneath anode, orientation as in cell; left: experiment: 004-SP7-4-01, cell 181, Anode T, with 5.48% C in frozen bath layer, anode was set too low, carbon dust level 1 or 2, no skimming, 4 h duration, carbon particles included are up to 25 mm in size, carbon in bath sample from tap hole: 0.0401% C; right: 025-Sp6-2-01, cell 174, anode C, with 6.29% C in frozen bath layer sample and 0.0318% C in bath sample taken in tap hole, dust index 3, no Skimming, normal height, 2 h duration

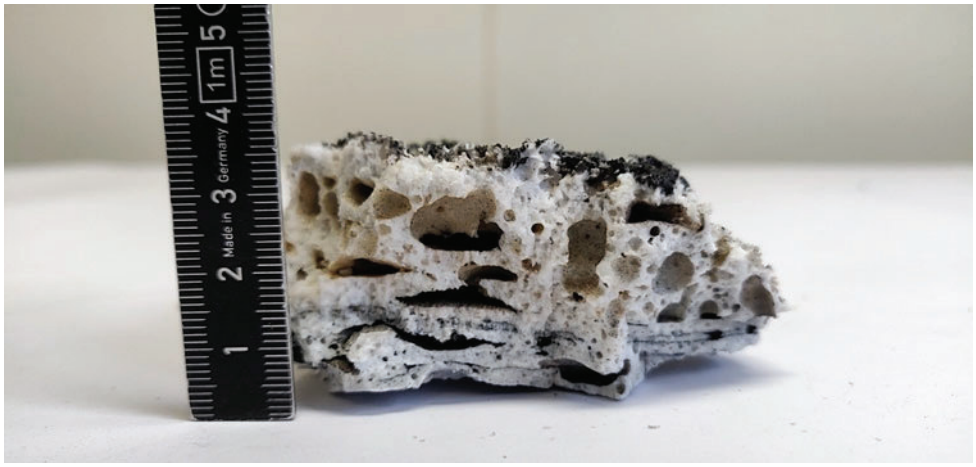

Fig. 7 Sample orientation as in cell, experiment 015-Sp1-4-02, cell 264, Anode K, duration: 4 h, skimming, correct height, carbon dust level 1-2, carbon in spike: 0.23% C, in bath sample: 0.0232% C. The samples two layers and especially in the upper layer high amounts of porosity. The lower layer shows fine carbon dust particles

carbon inclusions. The carbon content for the sample shown in Fig. 7 is at 0.23% C in the frozen bath sample and 0.0232% C during sampling in the tap hole.

The expectation, that parts of the frozen bath underneath the anodes is anode cover material dropped into the bath during anode change, was not observed during the experiments. The highest alumina concentration in the frozen bath samples was 7.5%. We would expect a content of approximately 40–60% Al_2O_3 for anode cover material.

The visual inspection of the freeze samples does suggest that the use of a pacman reduces the number of larger carbon particles, but the fine carbon dust can still be found underneath the anode.

The mechanism for the layering, which was evident in 11 of 30 (11 have two layers, 9 have one layer, for 10 experiments, there are no samples available) experiments, could be an initial layer freezing as soon as the anode touches the electrolyte, while the second layer freezes afterwards and into the metal pad. The amount of larger carbon particles appears likely to be related to the skimming action. The fine carbon dust particles cannot be taken out with skimming.

Chemical Composition of Bath Samples Underneath the Anode

Figure 8 shows the carbon content analysed with the LECO method compared to the carbon dust index assessed at the tap hole of the cell. One might expect a correlation between the carbon content and the carbon dust level assessment at the tap hole. However, the data does not confirm the expectation. The reliability of the carbon dust levels assessed in the tap hole is not robust during the experiments. Looking at the analysis of the bath samples taken at the tap hole, the highest carbon amounts are in Level 2 cells. The largest source of variation in the results is the heterogeneous

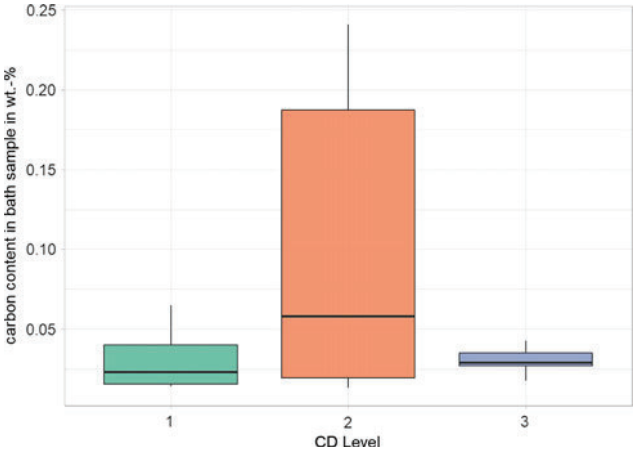

Fig. 8 Carbon Dust Level 1, 2 and 3 show different results in the actual measured bath samples taken at the tap hole. The largest variation can be observed with the level 2 cells, with values between 0.0131 and 0.241% C. (Color figure online)

distribution of carbon throughout the cell. All the tap hole bath samples have carbon values measured in the bath below 0.24%, which is lower than data published.

Conclusions

Thirty experiments have been conducted at the TRIMET Hamburg smelter in order to assess the hypothesis that a certain set of parameters during anode change, including the dust level in the cell, can lead to a spike formation and that these spikes form within the first hours after anode change.

The skimming action during anode change can reduce the amount of big carbon particles from old anodes. However, it does not appear to reduce the amount of fine carbon particles, also referred to as carbon dust.

The frozen bath under the anodes, checked after up to four hours, have a different appearance depending on the parameters used for anode change. The main driver for the thickness of frozen bath underneath the anodes are the use of pacman for skimming and the height of the newly set anode. Anodes, that are set too low, have a thicker freeze than normal set anodes. Anodes with no skimming actions during anode change show a thicker freeze under the anodes.

The carbon dust index observed at the tap hole appears not to be representative of the dust level in the anode hole in these experiments, or perhaps for the complete cell. If this is the case for the P19 Hamburg cell, the problem of tap hole dust observations might be even worse for bigger cells. The heterogeneous carbon distribution in the bath should be investigated.

During the experiments, no spike formed underneath the anodes within the first 8 h, and the anodes did not form a spike within the next 27 days until their scheduled next anode change. Anodes did not show any residual frozen bath on the working surface 8 h after anode setting.

References

1. L. Bugnion and J.-C. Fischer, 'Effect of carbon dust on the electrical resistivity of cryolite bath', in *Light Metals 2016*, Springer, 2016, pp. 587–591.
2. H. Gudmundsson, 'Improving anode cover material quality at Nordural—Quality tools and measures', in *Essential Readings in Light Metals*, Springer, 2016, pp. 639–644.
3. S. Pietrzyk and J. Thonstad, 'Influence of carbon dust in the electrolyte on aluminium electrolysis parameters', *ICSOBA Proc.*, pp. 659–666, 2015.
4. E. Cutshall, 'Influence of anode baking temperature and current density upon carbon sloughing', *Light Met. 1986*, vol. 2, pp. 629–637, 1986.
5. V. Buzunov, V. Shestakov, P. Polyakov, V. Tikhomirov, and S. Resmyatov, 'Statistical analysis of operation of electrolyzers for aluminum production', *Tsvetn Met*, vol. 6, pp. 30–33, 1994.
6. T. Foosnæs, T. Naterstad, M. Bruheim, and K. Grjotheim, 'Light Metals 1986', in *115th Annual Meeting of AIME, New Orleans, LA*, 1986, pp. 729–38.
7. P. Polyakov, A. Vlasov, Y. G. Mikhalev, and V. Yanov, 'On Cone Formation on Burnt Anode Face in Aluminum Electrolyzers', *Metallurgist*, vol. 60, no. 9–10, pp. 1087–1093, 2017.
8. R. C. Perruchoud, K. L. Hulse, W. K. Fischer, W. Schmidt-Hatting, and U. Heinzmann, 'Dust generation and accumulation for changing anode quality and cell parameters', *Light Metals 1999, Warrendale PA*, pp. 509–516, 1999.
9. B. Sadler and B. Welch, 'Reducing carbon dust?–needs and possible directions', in *9th Australasian Aluminium Smelting Technology Conference and Workshops, Terrigal, Australia*, 2007, p. 1.
10. J. Lhuissier, L. Bezamanifary, M. Gendre, and M.-J. Chollier, 'Use of under-calcined coke for the production of low reactivity anodes', in *Essential Readings in Light Metals*, Springer, 2016, pp. 109–113.
11. W. K. Fischer, F. Keller, and R. Perruchoud, 'Interdependence between anode net consumption and pot design, pot operating parameters and anode properties', *Light Met.*, vol. 681, 1991.
12. A. Zoukel, P. Chartrand, and G. Soucy, 'Study of aluminum carbide formation in Hall-Heroult electrolytic cells', *Light Met.*, vol. 2009, pp. 1123–1128, 2009.
13. H. Gudbrandsen, Sterten, and R. Ødegård, 'Cathodic dissolution of carbon in cryolitic melts', *Light Met.*, 1992, pp. 521–528, 1992.
14. O. E. Frosta, 'Anode Cover Material - Impact on anodes', presented at the 6th Icelandic Rodding Shop Conference, 2014.
15. M. W. Meier, R. C. Perruchoud, and W. K. Fischer, 'Production and performance of slotted anodes', *Light Met.*, pp. 277–282, 2007.
16. A. Fitchett, D. Morgan, and B. Welch, 'The reduction in anode airburn with protective covers', in *Essential Readings in Light Metals*, Springer, 2016, pp. 663–666.
17. N. Bird, B. McEnaney, and B. Sadler, 'Some Practical Consequence of Analyses of the Carboxy and Airburn Reactions of Anode Carbons', *Light Met. 1990*, pp. 467–471, 1990.
18. W. Fischer and R. Perruchoud, 'Factors Influencing the Carboxy- and Air-Reactivity Behavior of Prebaked Anodes in Hall–Heroult Cells', *Light Met. 1986*, vol. 2, pp. 575–580, 1986.
19. D. Brooks and V. Bullough, 'Factors in the design of reduction cell anodes', *Light Met. 1984*, pp. 961–976, 1984.

20. R. W. Peterson, 'Temperature and voltage measurements in Hall cell anodes', in *Essential Readings in Light Metals*, Springer, 2016, pp. 500–508.
21. F. Aune, M. Bugge, H. Kvande, T. Ringstad, and S. Rolseth, 'Thermal effects by anode changing in prebake reduction cells', Minerals, Metals and Materials Society, Warrendale, PA (United States), 1996.
22. B. Sadler and S. Algie, 'Macrostructural assessment of sub-surface carboxy attack in anodes', in *JOURNAL OF METALS*, 1988, vol. 40, pp. 36–36.
23. B. Patra and A. Palchowdhury, 'Improvement in oxidation Behaviour of Prebake anodes used in NALCO smelter plant', 2017.
24. A. Jassim, N. Al Jabri, S. A. Rabbaa, E. G. Mofor, and J. Jamal, 'Innovative Anode Coating Technology to Reduce Anode Carbon Consumption in Aluminum Electrolysis Cells', in *Light Metals 2019*, Springer, 2019, pp. 745–752.
25. R. Odegard and H. Gudbrandsen, 'A Study of spikes from industrial hall-herould anodes', *Aluminium*, vol. 68, no. 1, pp. 56–59, 1992.
26. B. A. Sadler, 'Critical issues in anode production and quality to avoid anode performance problems', 2015.
27. R. Ødegård and S. H. Avard Midtlyng, 'Electrochemical and chemical reactivity of carbon electrodeposited from cryolitic melts containing aluminum carbide', *J. Electrochem. Soc.*, vol. 138, no. 9, pp. 2612–2617, 1991.
28. K. Solbu, 'Study on the deformation of prebaked anodes in aluminium electrolysis', Diploma thesis, Institute for Material Technology and Technical Electrochemistry, Norway's University of Technical and Natural Sciences, NTNU, Trondheim, 1999.
29. A. T. Tabereaux, 'Maximum anode effect voltage', *Light Met.*, vol. 207, pp. 405–410, 2007.
30. W. Kristensen, G. Höskuldsson, and O. Jonsson, 'Improvements in Smelter Performance through operating practices and process control', in *Proceedings of the 8th Australasian Aluminium Smelting Technology Conference and Worskhop, Yeppoon, Australia*, 2004, pp. 3–8.
31. K. Khaji and M. Al Qassemi, 'The Role of Anode Manufacturing Processes in Net Carbon Consumption', *Metals*, vol. 6, no. 6, p. 128, 2016.
32. K. Grjotheim, *Introduction to aluminium electrolysis: understanding the Hall-Hérloult process*. Aluminium-Verlag, 1993.
33. M. Ali and A. Omran, 'Anode spike formation in prebaked aluminium reduction cells', *Al-Azhar Univ. Eng. J. JAUES Vol 7 No 4 Dec*, p. 29, 2012.
34. N. Wai-Poi, B. Rolofs, and C. A. Voerde, 'Impact of energy management and superheat on anode spike formation', *Light Met.*, pp. 535–540, 2001.
35. J. Antille and R. Von Kaenel, 'Using a magnetohydrodynamic model to analyze pot stability in order to identify an abnormal operating condition', in *Essential Readings in Light Metals*, Springer, 2016, pp. 367–372.
36. H. Gudmundsson, 'Anode Dusting from a Potroom Perspective at Nordural and Correlation with Anode Properties', in *Light Metals 2011*, Springer, 2011, pp. 471–476.
37. M. P. Taylor, A. Mulder, M. J. Hautus, J. J. Chen, and M. Stam, 'Analysis of human work decisions in an aluminium smelter', *Int. J. Decis. Sci. Risk Manag.*, vol. 2, no. 1–2, pp. 46–65, 2010.
38. V. Potocnik, A. Arkhipov, N. Ahli, and A. Alzarooni, 'Measurement of DC busbar currents in aluminium smelters', in *Proceedings of 35 th International ICSOBA Conference, Hamburg, Germany, Travaux*, 2017, vol. 46, pp. 1113–1128.
39. V. Gusberti, D. S. Severo, A. F. Schneider, E. C. Pinto, and A. C. Vilela, 'Modeling the effect of the anode change sequence with a non-linear shallow water stability model', *Light Met.*, pp. 157–164, 2007.
40. M. Jensen, K. Kalgraf, T. Nordbo, and T. Pedersen, 'ACD measurement and theory', in *Light Metals*, TMS San Francisco, CA, 2009, pp. 455–459.
41. M. W. Meier, *Anodes—From the raw materials to the pot performance—Proceedings of 8th International Training Course 2018*, 2018.